UNIVERSITY OF BIRMINGHAM

Research at Birmingham

Experimental behaviour of stainless steel bolted t-stub connections under monotonic loading

Yuan, Huanxin; Hu, S; Du, X.X.; Cheng, X.Y.; Theofanous, Marios

Link to publication on Research at Birmingham portal

Highlights

- Monotonic loading tests on 27 stainless steel bolted T-stub connections.

- The three typical failure mechanisms are observed for stainless steel T-stubs.

- Key parameters including bolt preload, material grade, flange thickness and bolt diameter are analysed.

- Evaluation of current design methods for predicting tension resistances of bolted T-stubs.

Experimental behaviour of stainless steel bolted T-stub connections under monotonic loading

H.X. Yuan[a, *], S. Hu[a], X.X. Du[a], L. Yang[b], X.Y. Cheng[a], M. Theofanous[c]

[a] *School of Civil Engineering, Wuhan University, Wuhan 430072, PR China*

[b] *The College of Architecture and Civil Engineering, Beijing University of Technology, Beijing 100124, PR China*

[c] *Department of Civil Engineering, University of Birmingham, Birmingham B15 2TT, United Kingdom*

Corresponding author:

Dr Huanxin Yuan, School of Civil Engineering, Wuhan University, Wuhan 430072, China. Email: yuanhx@whu.edu.cn

Abstract: A comprehensive experimental study on structural behaviour of stainless steel bolted T-stub connections is presented in this paper. A total of 27 stainless steel bolted T-stubs with various geometric configurations were fabricated from hot-rolled stainless steel plates and assembled with stainless steel bolts. Two stainless steel grades – austenitic EN 1.4301 and duplex EN 1.4462, and two other types of stainless steel bolts – A4-70 and A4-80, were introduced in the experimental programme. Tensile coupon tests were performed to determine the material properties of the stainless steel plates and bolts. The bolted T-stub specimens were tested under monotonic loading, and ultimate resistances, plastic deformation capacities and failure modes were obtained. Based on the experimental results, the existing design methods for predicting tension resistances of the bolted T-stub connections, including design provisions in EN 1993-1-8, the continuous strength method (CSM), AISC manual and JGJ 82 and other design formulae for T-stubs with four bolts per row, were all evaluated. It was indicated that all the existing design methods provided generally conservative predictions for stainless steel bolted T-stub connections.

Keywords: Stainless steel; T-stub; Bolted connections; Experiments; Tension resistance

1. Introduction

Following the component approach provided in EN 1993-1-8 [1], the bolted beam-to-column connections in steel structures can be modelled as an assembly of basic components, where the column flange in bending, end-plate in bending, flange cleat in bending and base plate in bending under tension can be represented by an equivalent T-stub in tension [2-4]. The structural behaviour of bolted T-stubs including the resistance, stiffness and deformation capacity, would be of great importance to design of bolted beam-to-column connections. A series of theoretical and experimental studies have been carried out to explore the inherent load-carrying mechanism and the prying effects, and corresponding design methods by considering the effect of the key parameters have been reported [5-11]. It was concluded that both the flexural strength of the flange and the tensile strength of the bolt contributed to the tension resistance and failure mechanism of the T-stub connections [12,13]. There were three typical failure modes for carbon steel T-stub connections, while these might be strongly affected by the material properties of the adopted structural material [14,15].

Though the use of stainless steels in structural applications has been popularised by their prominent corrosion resistance and architectural appearance, special attention should be paid to structural design accounting for the nonlinear material behaviour [16,17]. Comprehensive studies on structural stainless steel members involving cold-formed sections [18-21], hot-rolled sections [22] and welded sections [23-25] have been conducted by many researchers. Recent experimental and numerical studies on stainless steel bolted connections and beam-to-column joints have been carried out and reported in Ref. [26-28]. It has been found that separate treatment in structural design is required due to the absence of a sharp yield point, considerable strain hardening and high ductility [29,30].

Regarding the structural behaviour of stainless steel bolted T-stub connections, the material nonlinearity and strain hardening may result in significant changes of the load-carrying behaviour. Bouchaïr et al. [31] conducted numerical studies on the resistance and ductility by considering the prying effects, still publically reported experiments on this component are scarce. Hence, the aim of the present paper involves providing test data of such components, and assessing the applicability of existing design methods.

The experimental programme consisting of 27 stainless steel bolted T-stubs was carried out, and two stainless steel grades and two types of stainless steel bolts were introduced into this study. The stainless steel bolted T-stub connections were tested under monotonic loading, revealing the resistance, deformation capacity and failure mechanism, which were further utilised to evaluate the existing design methods.

2. T-stub test specimens

2.1. Specimens geometry

The stainless steel T-stubs comprised two hot-rolled plates with the same thickness – the web and the flange, which were welded together by two fillet welds. A total of 27 T-stub test specimens with various geometric configurations were fabricated and fastened through the flanges by using stainless steel bolts. Two stainless steel grades – austenitic EN 1.4301 and duplex EN 1.4462, and two other types of stainless steel bolts – A4-70 and A4-80, were involved in the experimental programme. The designation of bolts indicates that they are made of austenitic stainless steels (steel grade A4) and the minimum tensile strengths are 700 MPa and 800 MPa for A4-70 and A4-80, respectively [32]. In addition to the plate material grades and bolt types, two nominal plate thicknesses (8 mm and 12 mm), two bolt diameters (12 mm and 16 mm) and three different configurations of bolts (one bolt, two bolts and four bolts per row) have been considered. The test specimens were designed to achieve the three possible failure modes according to EN 1993-1-8 [1]. Meanwhile, the specimens are denoted as T-S, T-D and T-F in according with the configurations of the bolts (see Fig. 1), and the average measured dimensions of the T-stub test specimens are tabulated in Table 1, in which d_b is the nominal bolt diameter and h_f is the fillet weld size (weld leg length), while other geometric symbols are defined in Fig. 1. The fillet weld size h_f was selected as 5 mm and 6 mm for plate thickness of 8 mm and 12 mm, respectively. Two different levels of bolt preloading forces were introduced herein. Specifically, the design preload for A4-70 bolts was taken as 80% of the nominal bolt yield resistance, while the preload for A4-80 bolts was equal to 60% of the corresponding bolt yield resistance. The tightening process for preloaded bolts was performed by means of a calibrated wrench, and tightening for non-preloaded bolts (adopted in specimens S9, D8 and F10) was brought to a snug tight condition, with special care being given to avoid over-tightening. The actual preloads of the T-stub specimens monitored by circular load cells are summarised in Table 1. The circular load cells with a capacity 200 kN were calibrated by means of a 1000 kN capacity standard dynamometer. Moreover, the peak value of the bolt preload was taken as the stable value after tightening for a few seconds to take into account the possible overshoot effect.

2.2. Material properties

The material properties of stainless steel plates and bolts were experimentally determined prior to the monotonic loading tests. As described above, two stainless steel grades (austenitic EN 1.4301 and duplex EN 1.4462) for plates and two types of stainless steel bolts were considered in this study. Standard tensile coupon tests were therefore carried out for each kind of plates and bolts by referring to the Chinese testing standard [33]. Rectangular and round tensile coupons were prepared for the stainless steel plates and bolts, respectively. The rectangular tensile coupons were cut directly from the original hot-rolled plates by means of a wire-cutting technique, while the round tensile coupons with threaded ends were machined from the bolts, as shown in Fig. 2. There were a total of 12 rectangular tensile coupons and 12 round tensile coupons, since each stainless steel alloy had two different plate thicknesses and each type of stainless steel bolts had two different nominal bolt diameters, and three repeated coupons were tested for each case.

The tensile coupons were all tested using a 300 kN capacity universal testing machine. For each rectangular tensile coupon, an extensometer and two orthogonal strain gauges were adopted, while for round tensile coupons, the same extensometer and two other unidirectional strain gauges were used in the tensile tests. The experimentally obtained stress-strain curves and average measured material properties of the stainless steel plates and bolts are presented in Fig. 3 and Table 2, where the following symbols are used: E_0 is the initial Young's modulus, v is the Poisson's ratio, $\sigma_{0.01}$, $\sigma_{0.2}$ and $\sigma_{1.0}$ are the 0.01%, 0.2% and 1% proof stresses, respectively, σ_u is the ultimate tensile stress, ε_u is the strain at the ultimate tensile stress (not obtained for all coupons due to the limited range of the extensometer), ε_f is the plastic strain at fracture, measured from the fractured tensile coupons as elongation over the standard gauge length, and n is the Ramberg–Osgood strain hardening exponent. The 0.2% proof stress is regarded as the nominal yield strength for stainless steel alloys due to the absence of a sharp yield point. It is shown that the austenitic grade EN 1.4301 exhibits relatively lower nominal yield strength but much more pronounced strain hardening capacity than the duplex grade EN 1.4462. Moreover, the obtained material properties of the A4-70 bolts conformed to the values provided in the standard [32], while both the average tensile strength and 0.2% proof strength of the A4-80 bolts were slightly lower than the specified minimum values. Besides, less considerable strain hardening capacities were observed for both types of stainless steel bolts than the stainless steel plates.

3. Monotonic loading tests

The monotonic loading tests on the bolted T-stub specimens were carried out by using a 600 kN hydraulic actuator with electrohydraulic servo controlling system. By means of the test setup shown in Fig. 4 (a), a uniform tension force was applied to the webs of the test specimens. A carbon steel rigid end plate with four bolt holes was welded to the web, thus enabling the bolted connection between the end plate and the hydraulic actuator, where four M20 high strength hexagon bolts were adopted to ensure the robustness of this connection. The flange of the T-stub specimens was connected to a rigid block, generating rigid support for T-stubs. Prior to testing, the alignment of the specimens was carefully conducted. The instrumentation configuration is shown in Fig. 4 (b) and (c). Two symmetrically installed linearly varying displacement transducers (LVDTs) were employed to measure the axial displacement at the web ends. Strain gauges with a specified accuracy of up to 20000 $\mu\varepsilon$ that attached to the flange were used to monitor material yielding. Specifically, a total of six strain gauges measured surface strains for the T-S and T-F specimens, while four strain gauges were used for the T-D specimens. Besides, calibrated load cells that measured the actual bolt preloads were further utilised to monitor the variation of bolt forces during testing.

The displacement control pattern was adopted throughout the loading process for all the test specimens. A consistent loading rate of 0.5 mm/min was applied during the linear stage, after which a constant displacement rate of 1.0 mm/min was used to control the monotonic tests. Both LVDTs and all strain gauges were recorded continuously. The loading process was terminated once a clear decline in axial load was observed or the fracture of bolts was achieved.

4. Discussion of experimental results

4.1. Failure modes

Typical failure modes of the tested specimens are shown in Fig. 5, displaying the plastic flexural deformation of flange and fracture of the bolts. It can be observed that the three possible failure modes according to EN 1993-1-8 [1] (see Fig. 6) for bolted T-stub connections have been achieved. Specifically, the type-1 mechanism is characterised by yielding of the flange plate through the formation of four plastic hinges, and the type-2 mechanism corresponds to the development of two hinges located at the flange-to-web connection accompanied by bolt failure, while the type-3 mechanism is defined by bolt failure in the absence of prying forces or flange yielding. In addition to the deformed shapes, the attached strain gauges were also utilised to determine the failure mechanism. The load versus

3

surface strain curves of specimen S5 and F3 are plotted in Fig. 7. It can be seen that the measured strain values from SG1 and SG2 of specimen S5 exceed the nominal yield strain of the flange material prior to the ultimate load, indicating the formation of four plastic hinges. While for specimen F3, only two plastic hinges can be observed from the measured strains from SG2 since the corresponding surface strains from SG1 lie below the yield strain. Combined with the deformed shapes of the tested specimens, it can therefore be concluded that the specimen S5 belongs to type-1 mechanism, while the specimen F3 corresponds to typical type-2 mechanism.

The failure mechanism of each tested T-stub specimen is given in Table 3, involving the three typical failure modes. Moreover, the effect of key parameters such as applied preload, material grade, flange thickness and bolt diameter on the obtained failure modes of the tested specimens is illustrated in Fig. 5. It is shown that the introduction of bolt preload has little effect on the failure mode of T-stub specimens according to Fig. 5 (a), while the variation of material grade, flange thickness and bolt diameter results in changes of the failure modes. The type-2 mechanism is attained for specimen D1 made of EN 1.4301 alloy, while the failure mode for specimen D5 with the same geometric dimensions and bolts belongs to type-3 mechanism due to the much higher nominal yield strength of EN 1.4462 alloy (Fig. 5 (b)). The failure modes of three test specimens – S5, D3 and F1 with nominal flange thickness of 8 mm correspond to type-1, type-2 and type-1 mechanisms, respectively, yet three other specimens – S3, D4 and F6 with nominal flange thickness of 12 mm display type-3, type-3 and type-2 mechanisms, respectively, indicating the significant influence of flange thickness, as shown in Fig. 5 (c). Due to the increased bolt diameter from M12 to M16, the type-3 mechanism obtained for specimens S4 and D2 has changed to type-2 mechanism for specimens S7 and D6, and the type-2 mechanism achieved by specimen F8 becomes type-1 for specimen F2, as presented in Fig. 5 (d). It can thus be concluded that the formation of failure mechanism of bolted T-stub connections is directly related to the choice of different combinations of material grade, flange thickness and bolt diameter. Besides, the bolt shear failure can be observed for tested specimens subject to type-1 and type-2 mechanism, which can be attributed to the fact that shear actions on the bolts become prevalent due to the presence of the connected rigid support.

4.2. Load-carrying behaviour and influence of the key parameters

The applied load was plotted versus the average value of axial displacement measured by the two symmetrically placed LVDTs, as shown in Fig. 8. The ultimate resistances and corresponding deformation capacities derived from the monotonic loading tests are summarised in Table 3, and the obtained ultimate resistances are also presented in Fig. 9, where detailed comparisons of the effect of the key parameters considered (i.e. applied bolt preload, flange thickness, bolt diameter, material grade) on the ultimate resistance of the T-stubs are depicted.

As mentioned above, three test specimens – S9, D8 and F10 were assembled with non-preloaded bolts, where the snug tight conditions were achieved. It can be found that the initial slope of the load versus displacement curve of the three specimens is much lower than the three other specimens – S2, D2 and F3 with preloaded bolts, implying the significantly increased initial stiffness owing to the bolt preloading, as illustrated in Fig. 8. However, it is shown that the introduction of bolt preloading has little effect on the ultimate resistance and deformation capacity of the T-stub connections (see Fig. 9 and Table 3). The effect of flange thickness can be examined by comparing three pairs of specimens – S3 and S5, D3 and D4, F1 and F6. The three specimens with nominal flange thickness of 12 mm exhibited higher ultimate resistances, yet accompanied by slightly lower deformation capacity. Meanwhile, three other pairs of specimens – S4 and S7, D2 and D6, F2 and F8, were used to observe the effect of bolt diameter. It can be seen that the specimens assembled with bolt diameter of 16 mm displayed much higher ultimate resistances than those with bolt diameter of 12 mm. Along with the increased flange plate thickness and bolt diameter, enhanced initial stiffness of the bolted T-stub connections would be achieved. Furthermore, two material grades of the flange were considered in this study, and it was observed that the test specimens made of EN 1.4301 alloy had similar ultimate resistances with those made of EN 1.4462 alloy but exhibited differences in the overall load-deformation response. In accordance with their stress-strain curves, specimens made of austenitic material exhibited earlier loss of stiffness but superior strain hardening compared to their duplex counterparts.

4

4.3. Prying force

The prying forces in the bolted T-stub connections develop due to the flexure of the flange and corresponding contact of the flange tips with the underlying rigid plates and increase the tension force experienced by the bolts. The prying forces can be determined by comparing the sum of the bolt forces as experimentally measured and the applied load [34]. The experimentally obtained bolt force versus applied load curves of the tested specimens are plotted in Fig. 10, where the prying forces can be taken as the offset distance between the curve and the diagonal line. It is shown that the prying forces gradually increase with the applied load owing to the increasing flexure. For the T-stub specimens assembled with preloaded bolts, the resulting plate compression counteracts the applied load, thus delaying the development of prying forces. Once the plate compression reduces to zero, rapidly increasing prying forces can be noticed. Moreover, it can also be found that the level of the bolt preloading has little effect on the magnitude of prying forces at the ultimate stage by referring to the bolt force versus applied load curves of the two pairs of specimens – S2 and S9, D2 and D8. Besides, the increase of the flange thickness reduces the magnitude of the prying forces, as observed from the curves of the other two pairs of specimens – S3 and S5, D3 and D4 due to the increase in flexural stiffness of the flange.

5. Evaluation of the existing design methods

The design methods for predicting the resistances of the bolted T-stub connections made of carbon steels have been provided in EN 1993-1-8 [1], where the design formulae taking into account the three typical failure modes can be applied for stainless steels since there are no special provisions given in EN 1993-1-4+A1 (2015) [35]. Meanwhile, the design provisions in AISC manual [36] and Chinese code JGJ 82 [37] are based on calculating the minimum required thickness of T-stub flange, and the resistances of T-stub connections can then be computed. Besides, the design provisions in EN 1993-1-8 were further extended by Demonceau et al. [38] to cover the design of T-stub connections with four bolts per horizontal row. In view of the rounded stress-strain relationship of stainless steel alloys, Afshan and Gardner [39] developed the continuous strength method (CSM) which employs an elastic, linear hardening material model, where the strain hardening slope is given in Eq. (1).

$$E_{sh} = \frac{\sigma_u - \sigma_{0.2}}{0.16\varepsilon_u - \varepsilon_y} \tag{1}$$

in which the ε_y it the elastic strain at the material 0.2% proof stress, $\varepsilon_y = \sigma_{0.2}/E_0$.

By introducing the material model in the CSM, the design formulae from EN 1993-1-8 and Demonceau et al. [38] were further computed to allow for exploitation of the significant strain hardening capacities of T-stub flanges. The design provisions in the three existing design standards, the CSM and the design proposal from Demonceau et al. were therefore evaluated by using the previously obtained test results, where all the partial safety factors were set equal to unity in the comparison.

According to EN 1993-1-8, the tension resistances of T-stubs should be determined by taking into account the prying effects, where the three typical failure modes corresponds to the schematic figures presented in Fig. 6. The design tension resistance can be calculated by Eqs. (2)-(4) assuming that the force applied to the T-stub flange by a bolt is uniformly spread under the washer instead of concentrated at the centre-line of the bolt. The design tension resistance should be taken as the smallest value for the three failure modes.

Type-1 $$F_{1,\,Rd} = \frac{(8n - 2e_w)M_{f,1,Rd}}{2mn - e_w(m+n)} \tag{2}$$

Type-2 $$F_{2,\,Rd} = \frac{2M_{f,2,Rd} + n\sum F_{t,Rd}}{m+n} \tag{3}$$

Type-3 $$F_{3,\,Rd} = \sum F_{t,Rd} \tag{4}$$

where $M_{f,1,Rd}$ and $M_{f,2,Rd}$ are the moment resistances of the T-stub flange corresponding to the type-1 and type-2

modes, respectively, e_w is equal to $d_w/4$ (d_w is the diameter of the washer), $F_{t,Rd}$ is the design tension resistance of a bolt, m and n are as indicated in Fig. 1.

Regarding the design resistances of the T-stubs with four bolts per row (T-F specimens, see Fig. 1), Demonceau et al. [38] proposed calculation methods based on the same three failure modes. Compared to the ordinary T-stubs with two bolts, the formulae for predicting the tension resistances for T-stubs with four bolts per row corresponding to the type-1 and type-3 modes (i.e., Eqs. (2) and (4)) can still be utilised, yet significant differences exist in the type-2 failure mode, leading to the following expression.

$$F_{2,Rd} = \min \left[\frac{2M_{f,2,Rd} + \frac{\sum F_{t,Rd}}{2} (\frac{n_1^2 + 2n_2^2 + 2n_1n_2}{n_1 + n_2})}{m + n_1 + n_2}, \frac{2M_{f,1,Rd} + \frac{\sum F_{t,Rd}}{2} n_1}{m + n_1} \right] \qquad (5)$$

where n_1 and n_2 are geometric dimensions as indicated in Fig. 1.

The design provisions in AISC manual provided the calculation formulae for determining the required thickness of T-stub flange. The minimum thickness t_{min} required to develop the available strength of the bolt with no prying effects can be determined according to Eq. (6), while the thickness of flange t_e required to ensure an acceptable combination of flange strength and bolt strength is given by Eq. (7) accounting for the possible prying effects.

$$t_{min} = \sqrt{\frac{4Be_2'}{pf_u}} \qquad (6)$$

$$t_e = \sqrt{\frac{4Te_2'}{pf_u(1 + \delta\alpha')}} \qquad (7)$$

where $B = 0.75F_uA$ is the axial tension force of a bolt, T is the axial tension force, e_2 is the distance from bolt centreline to the web (i.e., $e_2 = m + 0.8h_f$, m and $0.8h_f$ are as indicated in Fig. 1), e_2' is taken as $e_2 - d_b/2$, p is the tributary length, f_u is the specified minimum tensile strength of flange material.

Similar to the design formulae presented in the AISC manual, Eqs. (8) and (9) were introduced in the Chinese design code JGJ 82 to determine the corresponding minimum flange thickness t_{min} and the required thickness t_e, where the tensile strength was replaced with the material yield strength.

$$t_{ec} = \sqrt{\frac{4e_2N_t^b}{bf_y}} \qquad (8)$$

$$t_e = \sqrt{\frac{4e_2N_t}{\psi bf_y}} \qquad (9)$$

where N_t and N_t^b are the axial tension force and tension resistance of a bolt, respectively, b is as indicated in Fig. 1, ψ is the influence coefficient of prying forces, f_y is the material yield strength of the flange.

By referring to the design provisions from AISC manual and JGJ 82, the tension resistances of the tested T-stub specimens belonging to type-3 failure mode were calculated by the full exploitation of the bolt strength, and those categorised as type-1 and type-2 modes would be computed from the transformed expressions of Eqs. (7) and (9). It has to be noted that the above formulae were developed for the design of T-stubs made of carbon steels.

Based on the material properties of the stainless steel plates and bolts previously obtained from the coupon tensile tests (as listed in Table 2) and the measured geometric dimensions, a comparison of the predicted tension resistances from the existing design methods with the obtained experimental results is presented in Tables 4 and 5. It can be seen that all the existing design methods provide generally conservative predictions for the tested stainless steel bolted T-stub connections. According to the AISC manual, the mean value of $T_{u,AISC}/F_{u,Exp}$ for type T-S and T-D specimens is 0.80 with a corresponding standard deviation (St. dev) of 0.19. Though an underestimation of 20% in tension resistance was obtained, still the predicted tension resistances from the AISC manual are much closer to the experimental results than the other predictions, which may be attributed to the introduction of material tensile strength instead of yield strength. The design method in JGJ 82 offers the most conservative predictions for type T-S and T-D specimens that the ratio of $N_{tu,JGJ}/F_{u,Exp}$ is equal to 0.39, while the design provisions in EN 1993-1-8 predict 51% of the test resistances on average. For the ten type T-F specimens, the average ratio of predicted resistances by

Demonceau et al. to experimental results is 0.39, revealing overly conservative predictions. Combined with the design formulae from EN 1993-1-8 and Demonceau et al., the resistances of the T-stubs can also be determined by using the material model in the CSM. The mean value of $F_{u,CSM}/F_{u,Exp}$ is 0.71 for type T-S and T-D specimens, while the corresponding mean value for type T-F specimens is 0.54, revealing improved strength predictions compared to the traditional formulae from EN 1993-1-8 and Demonceau et al. Similar levels of conservatism were exhibited by EN 1993-1-8 in the prediction of the resistance of stainless steel beam-to-column joints [25], the failure of which was generally governed by the ultimate response of the stainless steel T-stub components of the connection.

6. Conclusions

The structural behaviour of stainless steel bolted T-stub connections has been experimentally investigated in this paper. Monotonic loading tests on a total of 27 stainless steel bolted T-stubs were carried out, involving two stainless steel grades, two types of stainless steel bolts and various geometric configurations. Prior to the loading tests, the material properties of stainless steel plates and bolts were determined by separate tensile coupon tests. The three typical failure modes of T-stub connections were achieved, and the resulted prying forces were also examined. The load-carrying behaviour were obtained and further utilised to explore the effect of the key parameters, including bolt preload, material grade, flange thickness and bolt diameter. It has been found that the introduction of bolt preload has little effect on the failure mode, ultimate resistance and deformation capacity, but generates significantly increased initial stiffness for the T-stub connections. The failure modes and tension resistances were affected by the other parameters that contributed to the flexural strength of the flange and the tensile strength of the bolt.

The obtained experimental results were therefore utilised to evaluate the existing design methods, including the design provisions in EN 1993-1-8, the CSM, AISC manual and JGJ 82 and design proposal by Demonceau et al. for T-stub connections with four bolts per row. It was concluded that the all existing design methods provide generally conservative predictions for the tested stainless steel bolted T-stub specimens. Due to the introduction of material tensile strength instead of yield strength, the predicted tension resistances from the AISC manual are much closer to the experimental results than the predictions from the other methods, though the material nonlinearity and prominent strain hardening of stainless steel plates and bolts have not been explicitly considered. Compared to the traditional design formulae from EN 1993-1-8 and Demonceau et al., improved predictions for tension resistances of T-stub connections could be achieved by introducing the material model in the CSM. The significant conservatism exhibited by the European and Chinese standards and the large standard deviation of the predictions of the AISC specifications some of which are unsafe for a small number of specimens indicate that the development of a design approach for stainless steel connections that accounts for the significant material nonlinearity and strain hardening exhibited by stainless steels is warranted.

References

[1] EN 1993-1-8, Eurocode 3: Design of steel structures−Part 1.8: Design of joints, CEN, 2005.
[2] Y.L. Yee, R.E. Melchers, Moment-rotation curves for bolted connections, J. Struct. Eng. ASCE 112 (3) (1986) 615–635.
[3] C. Faella, V. Piluso, G. Rizzano, Reliability of Eurocode 3 procedures for predicting beam-to-column joint behaviour, in: Proceedings of the 3rd Intl. Conf. on Steel and Aluminium Structures, Istanbul, May, 1995, 441-448.

[4] Y.J. Shi, S.L. Chan, Y.L. Wong, Modeling for moment-rotation characteristics for end-plate connections, J. Struct. Eng. ASCE 122 (11) (1996) 1300–1306.

[5] C. Faella, V. Piluso, G. Rizzano, Experimental analysis of bolted connections: snug versus preloaded bolts, J. Struct. Eng. ASCE 124 (7) (1998) 765–774.

[6] A.M.G. Coelho, F.S.K. Bijlaard, N. Gresnigt, L.S. da Silva, Experimental assessment of the behaviour of bolted T-stub connections made up of welded plates, J. Constr. Steel Res. 60 (2) (2004) 269–311.

[7] A.M.G. Coelho, L.S. da Silva, F.S.K. Bijlaard, Finite-element modeling of the nonlinear behavior of bolted T-stub connections, J. Struct. Eng. ASCE 132 (6) (2006) 918–928.

[8] V. Piluso, G, Rizzano, Experimental analysis and modelling of bolted T-stubs under cyclic loads, J. Constr. Steel Res. 64(6) (2008) 655–669.

[9] M. Latour, G. Rizzano, A. Santiago, L. Da Silva, Experimental analysis and mechanical modeling of T-stubs with four bolts per row, J. Constr. Steel Res. 101 (2014) 158–174.

[10] M.S. Zhao, C.K. Lee, S.P. Chiew, Tensile behavior of high performance structural steel T-stub joints, J. Constr. Steel Res. 122 (2016) 316–325.

[11] C. Chen, X. Zhang, M. Zhao, C.K. Lee, T.C. Fung, S.P. Chiew, Effects of welding on the tensile performance of high strength steel T-stub joints, Struct. 9 (2017) 70–78.

[12] V. Piluso, C. Faella, G. Rizzano, Ultimate behavior of bolted T-stubs. I: Theoretical model, J. Struct. Eng. ASCE 127 (6) (2001) 686–693.

[13] V. Piluso, C. Faella, G. Rizzano, Ultimate behavior of bolted T-stubs. II: Model validation, J. Struct. Eng. ASCE 127 (6) (2001) 694–704.

[14] G. De Matteis, A. Mandara, F.M. Mazzolani, T-stub aluminium joints: influence of behavioural parameters, Comput. Struct. 78 (1) (2000) 311–327.

[15] G. De Matteis, M. Brescia, A. Formisano, F.M. Mazzolani, Behaviour of welded aluminium T-stub joints under monotonic loading, Comput. Struct. 87 (15) (2009) 990–1002.

[16] L. Gardner, The use of stainless steel in structures, Progr. Struct. Eng. Mater. 7 (2) (2005) 45–55.

[17] N.R. Baddoo, Stainless steel in construction: a review of research, applications, challenges and opportunities, J. Constr. Steel Res. 64 (11) (2008) 1199–1206.

[18] K.J.R. Rasmussen, G.J. Hancock, Design of cold-formed stainless steel tubular members. I: Columns, J. Struct. Eng. ASCE 119 (8) (1993) 2349–2367.

[19] B. Young, W.M. Lui, Tests of cold-formed high strength stainless steel compression members, Thin-Walled Struct. 44 (2) (2006) 224–234.

[20] L. Gardner, D.A. Nethercot, Experiments on stainless steel hollow sections–Part 1: material and cross-sectional behaviour, J. Constr. Steel Res. 60 (9) (2004) 1291–1318.

[21] B.F. Zheng, X. Hua, G.P. Shu, Tests of cold-formed and welded stainless steel beam-columns, J. Constr. Steel Res. 111 (2015) 1–10.

[22] P.J. Bredenkamp, G.J. van den Berg, P. van der Merwe, The behaviour of hot-rolled and built-up stainless steel structural members, J. Constr. Steel Res. 46 (1998) 464.

[23] E. Real, E. Mirambell, I. Estrada, Shear response of stainless steel plate girders, Eng. Struct. 29 (7) (2007) 1626–1640.

[24] H.X. Yuan, Y.Q. Wang, L. Gardner, X.X. Du, Y.J. Shi, Local-overall interactive buckling behaviour of welded stainless steel I-section columns, J. Constr. Steel Res. 111 (2015) 75–87.

[25] X.W. Chen, H.X. Yuan, X.X. Du, Y. Zhao, J. Ye, L. Yang, Shear buckling behaviour of welded stainless steel plate girders with transverse stiffeners, Thin-Walled Struct. 122 (2018) 529–544.

[26] E.L. Salih, L. Gardner, D.A. Nethercot, Bearing failure in stainless steel bolted connections, Eng. Struct. 33 (2) (2011) 549-562.

[27] M. Elflah, M. Theofanous, S. Dirar, H.X. Yuan, Behaviour of stainless steel beam-to-column joints–Part 1: experimental investigation, J. Constr. Steel Res. Special Issue for the 5th International Stainless Steel Experts Seminar, submitted.

[28] M. Elflah, M. Theofanous, S. Dirar, Behaviour of stainless steel beam-to-column joints–Part 2: numerical modelling and design recommendations, J. Constr. Steel Res. Special Issue for the 5th International Stainless Steel Experts Seminar, submitted.

[29] O. Zhao, S. Afshan, L. Gardner, Structural response and continuous strength method design of slender stainless steel cross-sections, Eng. Struct. 140 (2017) 14–25.

[30] I. Arrayago, K.J.R. Rasmussen, E. Real, Full slenderness range DSM approach for stainless steel hollow cross-sections, J. Constr. Steel Res. 133 (2017) 156–166.

[31] A. Bouchaïr, J. Averseng, A. Abidelah, Analysis of the behaviour of stainless steel bolted connections, J. Constr. Steel Res. 64 (11) (2008) 1264–1274.

[32] EN ISO 3506-1, Mechanical properties of corrosion-resistant stainless steel fasteners−Part 1: Bolts, screws and studs, CEN, 2009.

[33] GB/T 228.1, Metallic materials−Tensile testing−Part 1: Method of test at room temperature, Standards Press of China, Beijing, 2011 (in Chinese).

[34] J.A. Swanson, R.T. Leon, Bolted steel connections: Tests on T-stub components, J. Struct. Eng. ASCE 126 (1) (2000) 50–56.

[35] EN 1993-1-4:2006+A1:2015, Eurocode 3: Design of steel structures–Part 1.4: General rules–Supplementary rules for stainless steels, CEN, 2015.

[36] AISC, Steel construction manual, 14th ed, 2011.

[37] JGJ 82, Technical specification for high strength bolt connections of steel structures, China Architecture and Building Press, Beijing 2011 (in Chinese).

[38] J.F. Demonceau, K. Weynand, J.P. Jaspart, C. Müller, Application of Eurocode 3 to steel connections with four bolts per horizontal row, in: Proceedings of the SDSS'Rio 2010 conference. Rio de Janeiro, 2010, 199–206.

[39] S. Afshan, L. Gardner, The continuous strength method for structural stainless steel design, Thin-Walled Struct. 68 (10) (2013) 42–49.
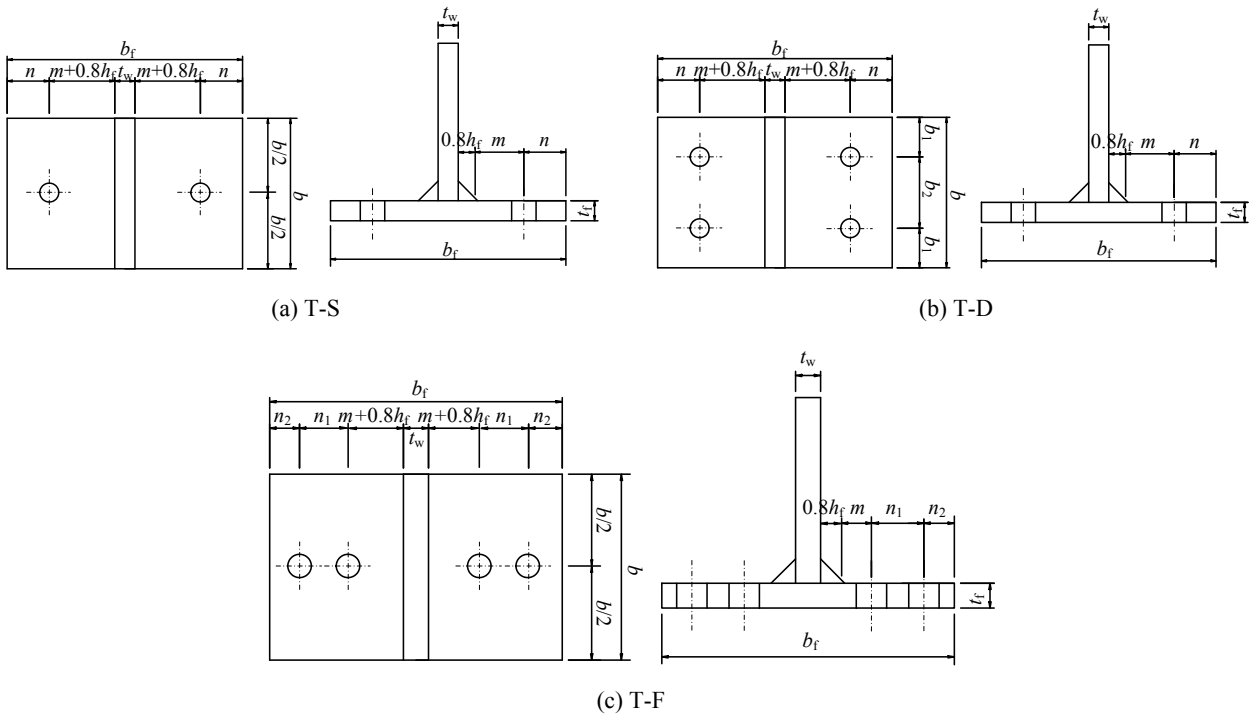
(a) T-S

(b) T-D

(c) T-F

Fig. 1. Geometric details of T-stub specimens.
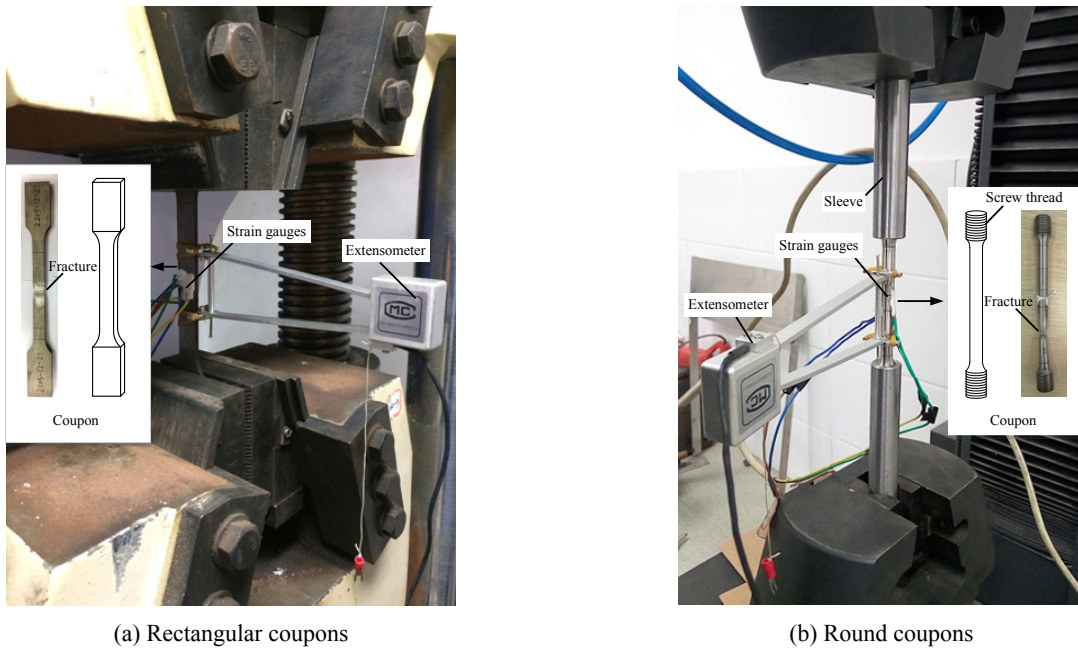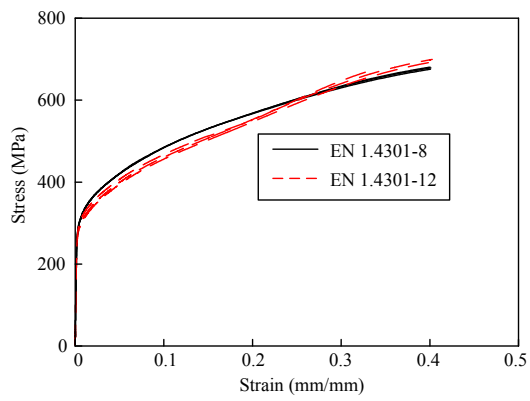

(a) Rectangular coupons
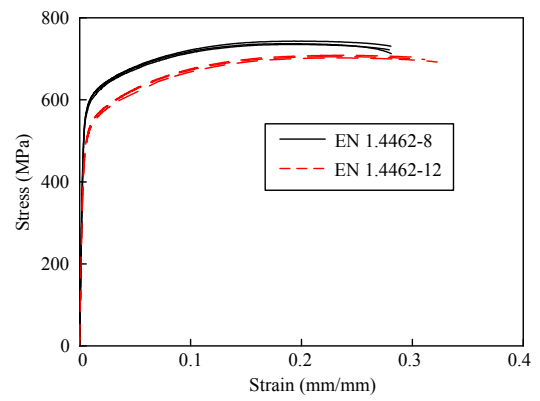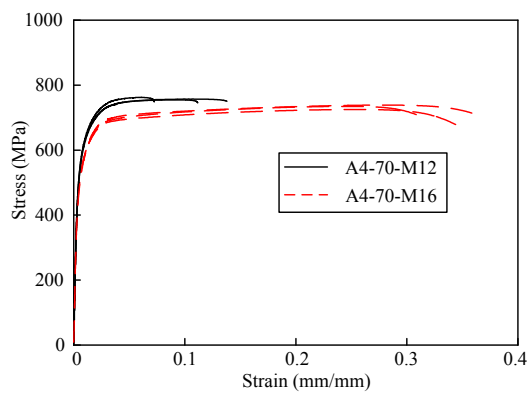
(b) Round coupons

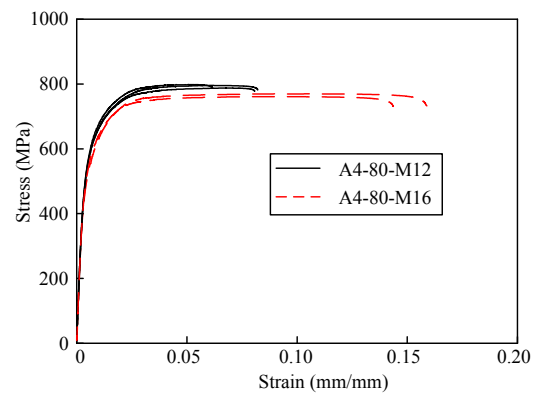**Fig. 2.** Tensile coupon tests of stainless steel plates and bolts.
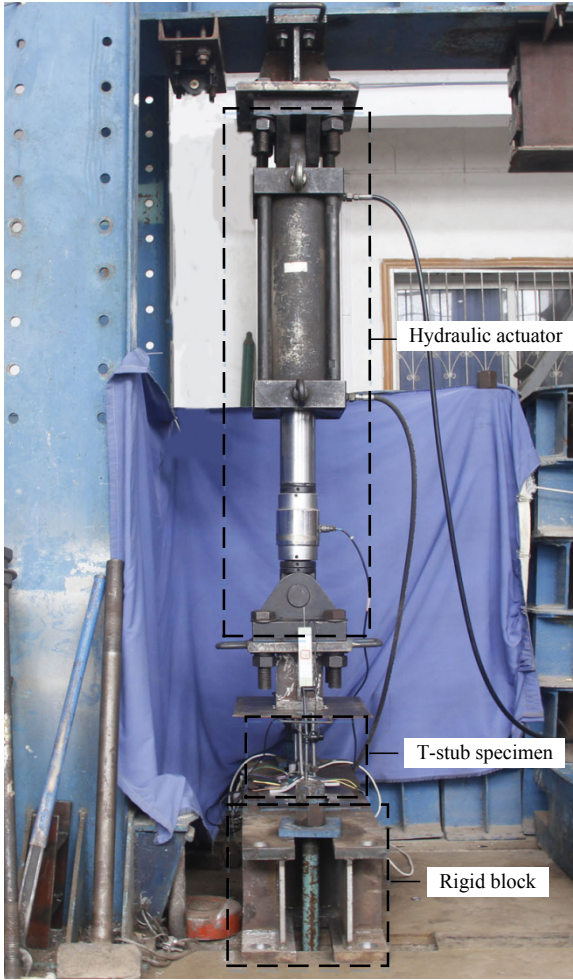
(a) EN 1.4301 plates

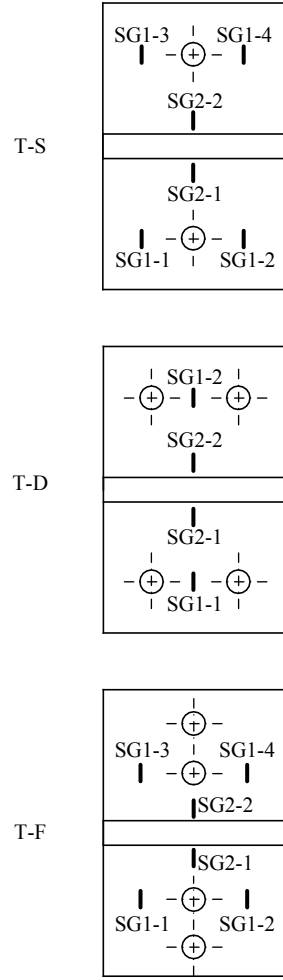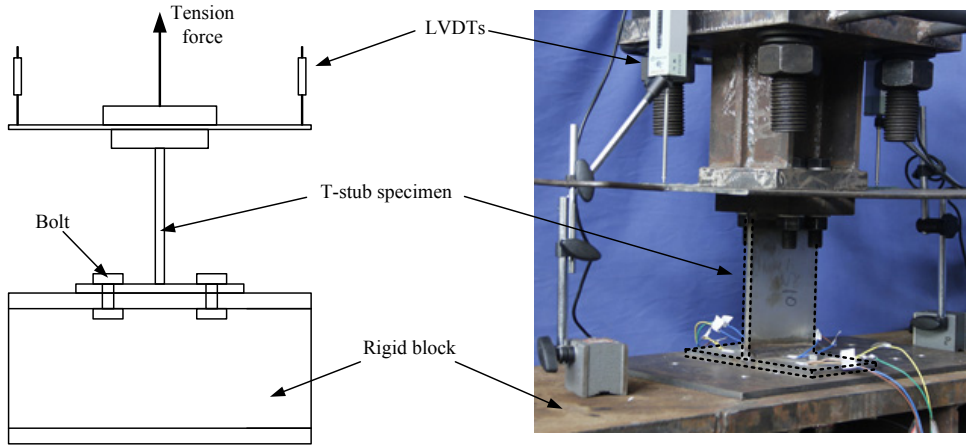(b) EN 1.4462 plates

(c) A4-70 bolts

(d) A4-80 bolts

Fig. 3. Stress-strain curves of tensile coupons from stainless steel plates and bolts.
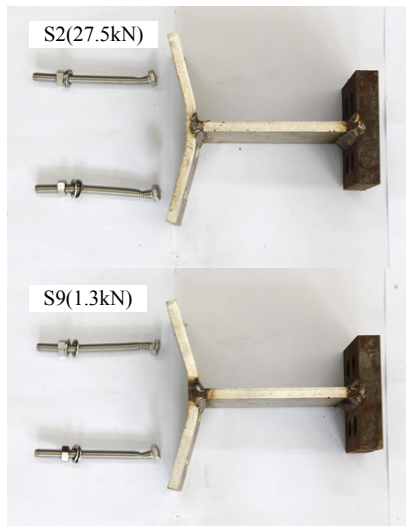
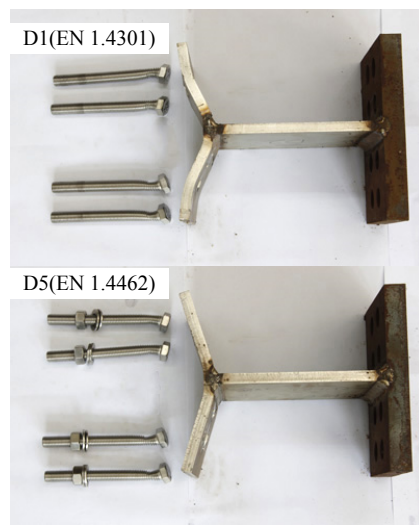(a) Test setup

(b) Configurations of strain gauges

Hydraulic actuator

T-stub specimen

Rigid block

T-S

SG1-3 SG1-4
SG2-2
SG2-1
SG1-1 SG1-2

T-D

SG1-2
SG2-2
SG2-1
SG1-1

T-F

SG1-3 SG1-4
SG2-2
SG2-1
SG1-1 SG1-2

Tension force

LVDTs

Bolt

T-stub specimen
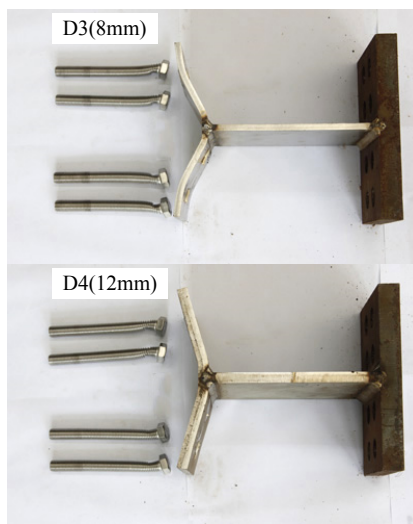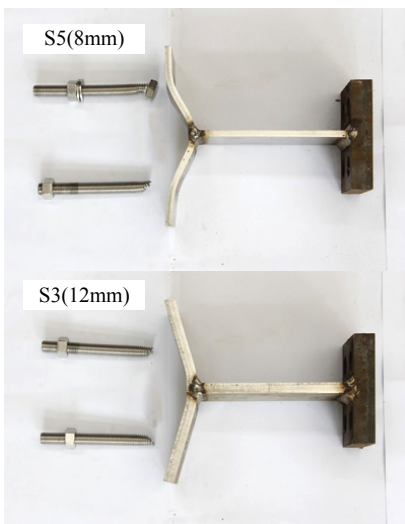
Rigid block

(c) Connection details

Fig. 4. The test setup and instrumentation configurations.
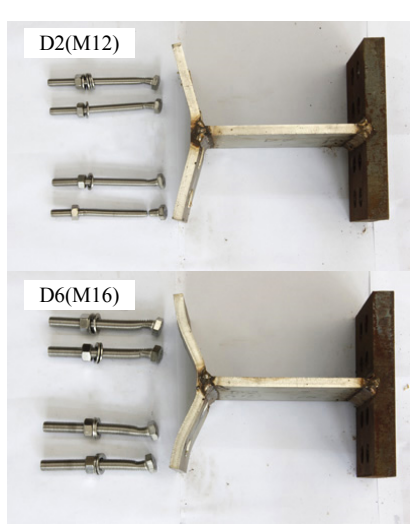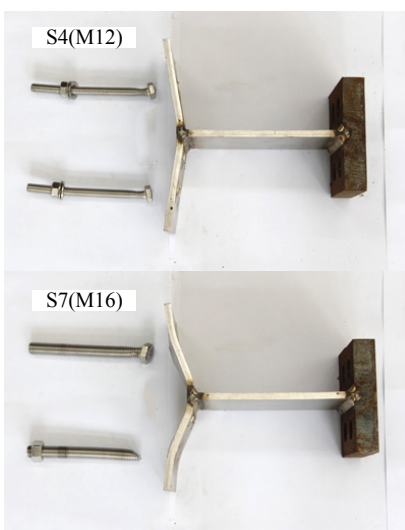
3

(a) Effect of bolt preload

(b) Effect of flange material grade
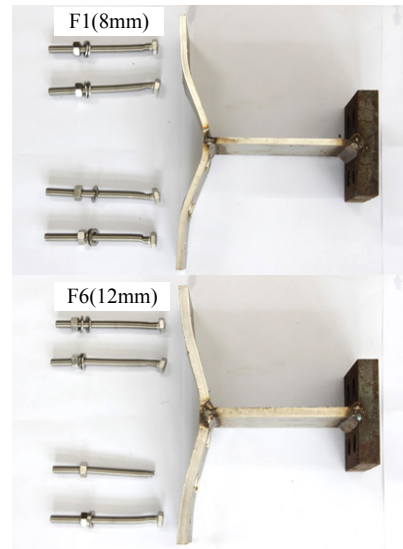
(c) Effect of flange thickness

(d) Effect of bolt diameter

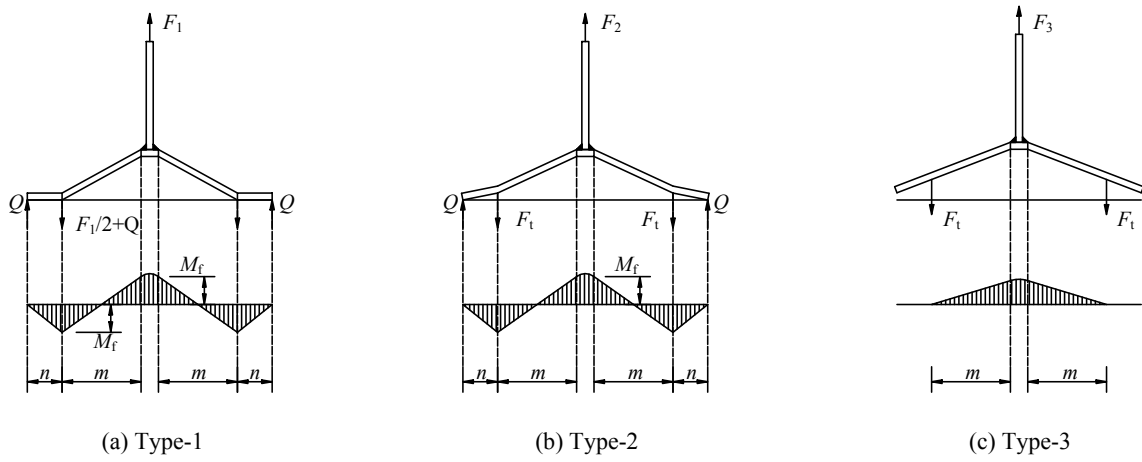**Fig. 5.** Failure modes of the tested T-stub specimens.

(a) Type-1 (b) Type-2 (c) Type-3

Fig. 6. Typical failure modes of T-stubs.

(a) Type-1 failure mode (b) Type-2 failure mode
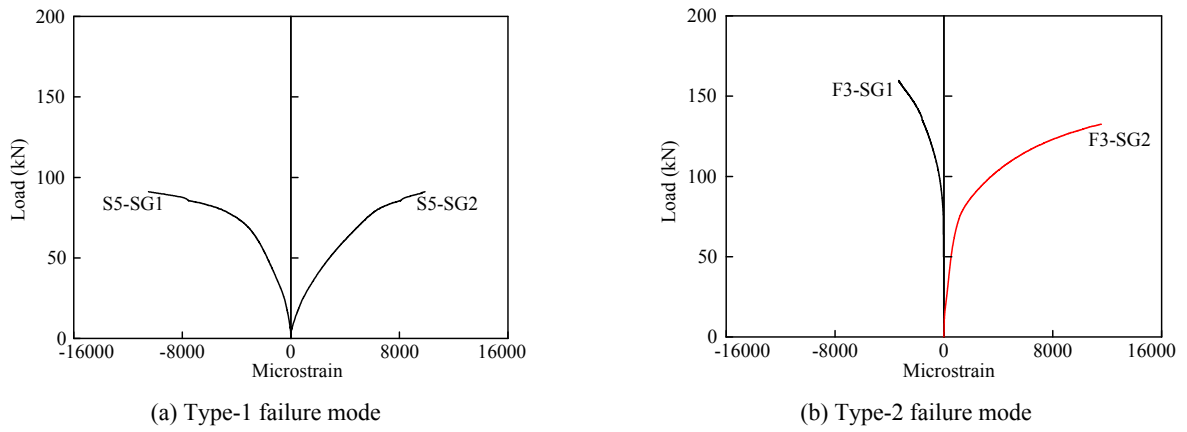
Fig. 7. Load-strain curves of the tested specimens.
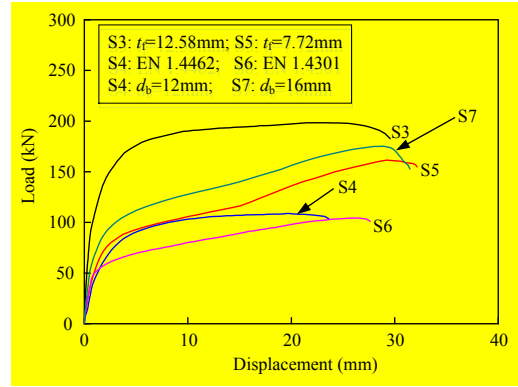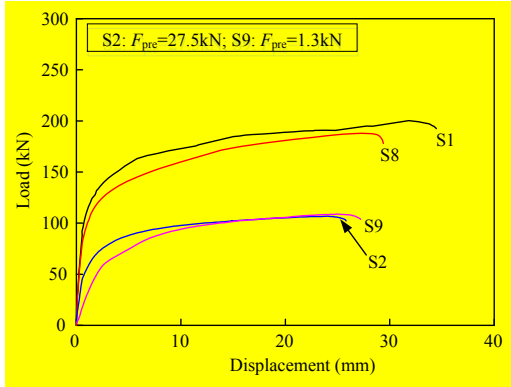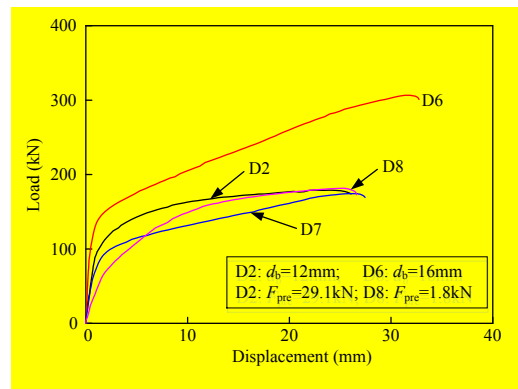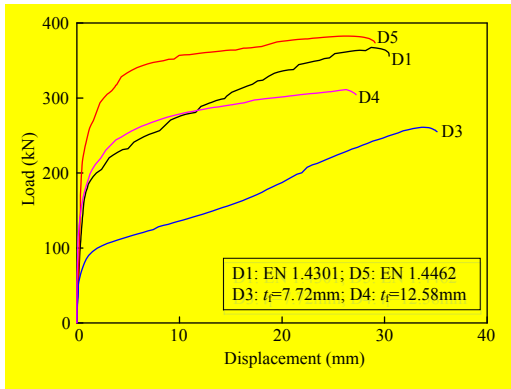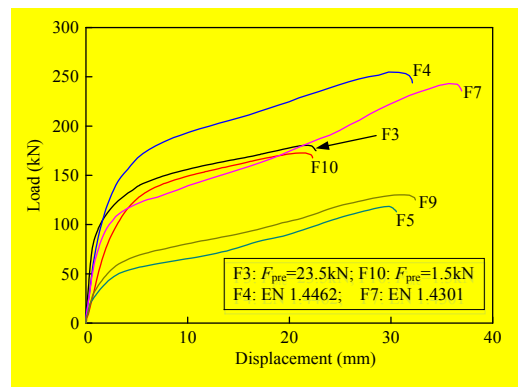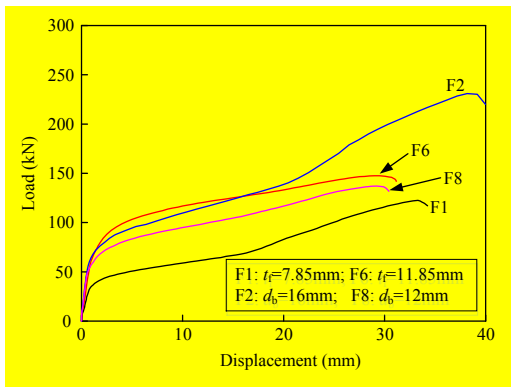
(a) Group T-S

(b) Group T-D

(c) Group T-F

Fig. 8. Load versus displacement curves of the tested specimens.

6

(a) Effect of bolt preload

(b) Effect of flange thickness

(c) Effect of bolt diameter

(d) Effect of flange material

Fig. 9. Comparison of ultimate resistances for the tested specimens.

(a) Group T-S

(b) Group T-D

Fig. 10. Bolt force versus applied load curves of tested specimens.

8

Table 1

Geometric dimensions and bolt preloads of T-stub specimens.

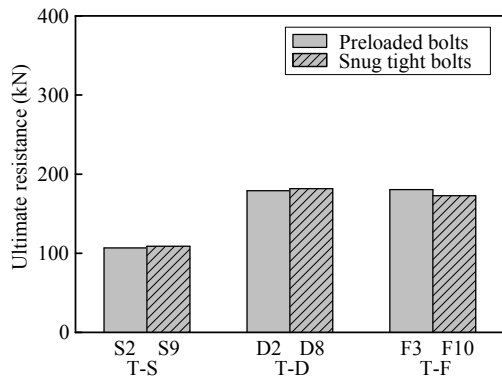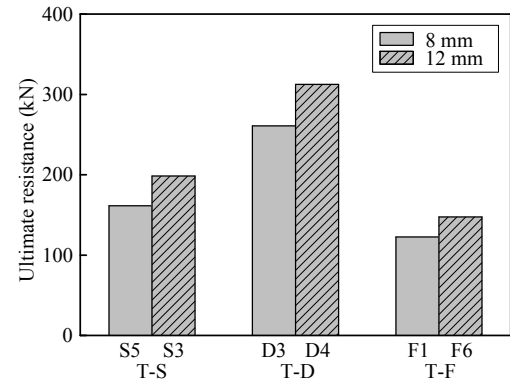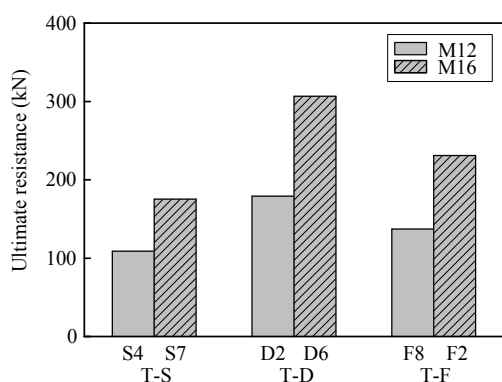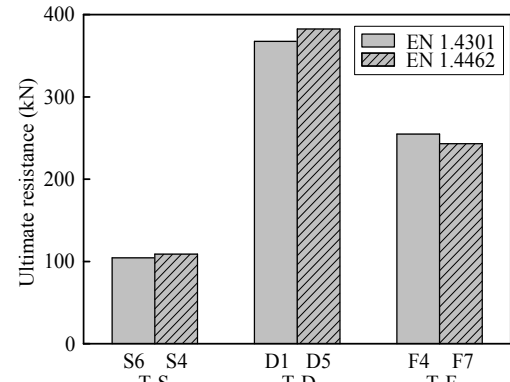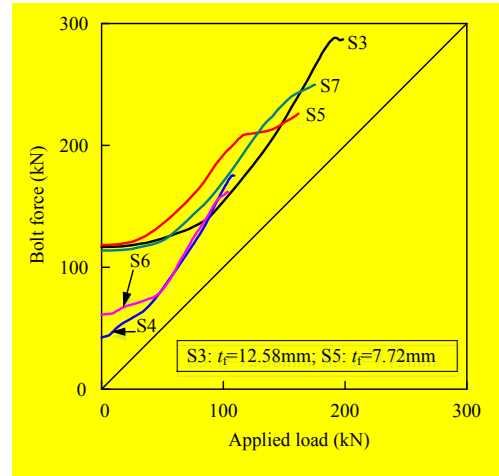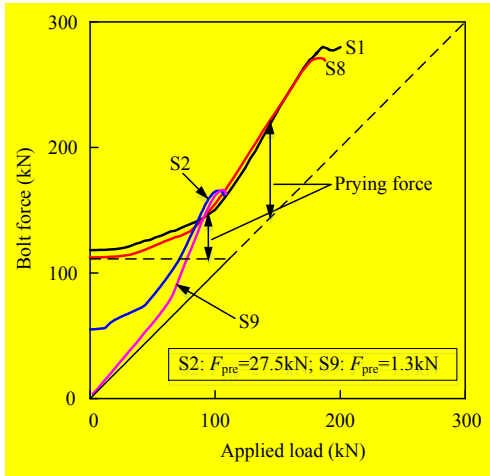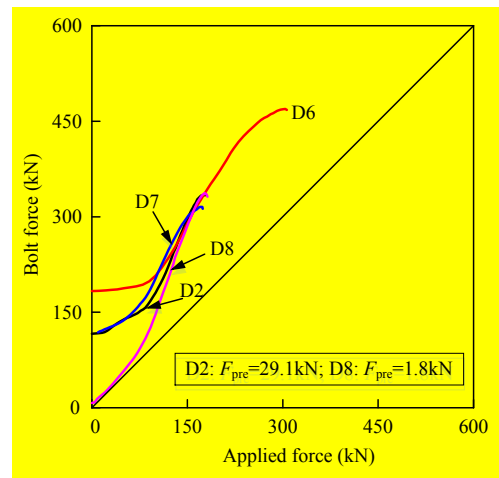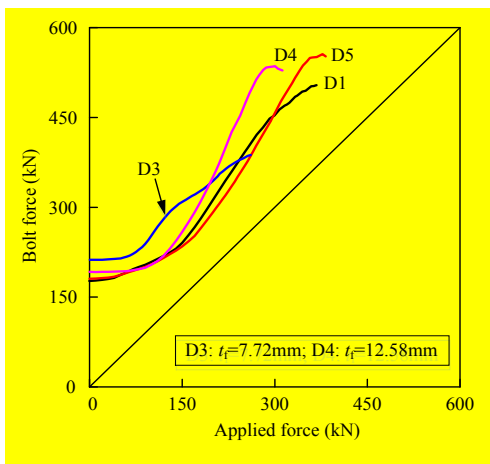| Type	Specimen	Material	Bolt	d_b	n_1	n_2	n	m	b_1	b_2	b	b_f	$t_f= t_w$	h_f	Bolt preload F_{pre} (kN)
T-S	S1	EN 1.4301	A4-70	16	-	-	50	50.2	-	-	120	222	11.85	6	59.1
	S2	EN 1.4301	A4-80	12	-	-	35	65.2	-	-	120	222	11.85	6	27.5
	S3	EN 1.4462	A4-80	16	-	-	50	50.2	-	-	90	222	12.58	6	58.3
	S4	EN 1.4462	A4-80	12	-	-	50	53.0	-	-	120	222	7.72	5	21.3
	S5	EN 1.4462	A4-80	16	-	-	50	53.0	-	-	90	222	7.72	5	59.1
	S6	EN 1.4301	A4-80	12	-	-	50	53.0	-	-	120	222	7.85	5	30.6
	S7	EN 1.4462	A4-80	16	-	-	50	53.0	-	-	120	222	7.72	5	56.9
	S8	EN 1.4301	A4-70	16	-	-	50	50.2	-	-	90	222	11.85	6	56.2
	S9	EN 1.4301	A4-80	12	-	-	35	65.2	-	-	120	222	11.85	6	1.3
T-D	D1	EN 1.4301	A4-70	16	-	-	50	50.2	40	70	150	222	11.85	6	44.3
	D2	EN 1.4301	A4-80	12	-	-	35	65.2	40	70	150	222	11.85	6	29.1
	D3	EN 1.4462	A4-70	16	-	-	35	68.0	40	70	150	222	7.72	5	53.1
	D4	EN 1.4462	A4-70	16	-	-	35	65.2	40	70	150	222	12.58	6	48.0
	D5	EN 1.4462	A4-70	16	-	-	50	50.2	40	70	150	222	12.58	6	45.2
	D6	EN 1.4301	A4-80	16	-	-	35	65.2	40	70	150	222	11.85	6	45.8
	D7	EN 1.4301	A4-80	12	-	-	35	65.2	28	54	110	222	11.85	6	29.4
	D8	EN 1.4301	A4-80	12	-	-	35	65.2	40	70	150	222	11.85	6	1.8
T-F	F1	EN 1.4301	A4-70	12	50	30	80	73.0	-	-	120	322	7.85	5	23.7
	F2	EN 1.4301	A4-70	16	50	30	80	70.2	-	-	90	322	11.85	6	36.8
	F3	EN 1.4301	A4-80	12	40	70	110	40.2	-	-	90	322	11.85	6	23.5
	F4	EN 1.4462	A4-80	16	50	30	80	70.2	-	-	120	322	12.58	6	39.6
	F5	EN 1.4462	A4-80	12	50	30	80	73.0	-	-	90	322	7.72	5	29.3
	F6	EN 1.4301	A4-70	12	50	30	80	70.2	-	-	120	322	11.85	6	23.9
	F7	EN 1.4301	A4-80	16	50	30	80	70.2	-	-	120	322	11.85	6	34.7
	F8	EN 1.4301	A4-70	12	50	30	80	70.2	-	-	90	322	11.85	6	25.8
	F9	EN 1.4462	A4-80	12	50	30	80	73.0	-	-	120	322	7.72	5	27.9
	F10	EN 1.4301	A4-80	12	40	70	110	40.2	-	-	90	322	11.85	6	1.5

All dimensions except the bolt preload are in mm.

Table 2

Measured material properties of stainless steel plates and bolts.

Stainless steel plates and bolts	Plate thickness or nominal bolt diameter (mm)	v	E_0 (MPa)	$\sigma_{0.01}$ (MPa)	$\sigma_{0.2}$ (MPa)	$\sigma_{1.0}$ (MPa)	σ_u (MPa)	ε_u (%)	ε_f (%)	n
EN 1.4301	7.85	0.257	180700	191.4	291.7	338.9	706.0	-	62.9	7.1
EN 1.4301	11.85	0.258	182800	184.7	280.4	319.1	719.6	-	57.7	7.2
EN 1.4462	7.72	0.207	188700	296.5	551.4	614.5	738.4	19.3	33.0	4.8
EN 1.4462	12.58	0.226	184000	227.8	464.6	552.8	705.3	23.3	37.4	4.2
A4-70	12	-	175400	273.8	522.6	667.1	758.1	8.5	36.5	4.6
A4-70	16	-	173000	283.8	484.6	622.7	732.7	26.0	44.9	5.6
A4-80	12	-	184500	271.5	553.9	710.4	794.0	5.9	29.7	4.2
A4-80	16	-	175300	300.7	524.4	682.3	765.4	9.8	33.4	5.4

Table 3

Failure modes and experimental results of tested T-stub specimens.

Specimen	Flange material grade	Bolt type	Failure mode	$F_{u,Exp}$ (kN)	$\Delta_{u,Exp}$ (mm)
S1	EN 1.4301	A4-70	3	200.2	31.8
S2	EN 1.4301	A4-80	3	106.8	23.9
S3	EN 1.4462	A4-80	3	198.4	21.5
S4	EN 1.4462	A4-80	3	108.9	19.7
S5	EN 1.4462	A4-80	1	161.6	29.2
S6	EN 1.4301	A4-80	2	104.3	26.0
S7	EN 1.4462	A4-80	2	175.2	28.9
S8	EN 1.4301	A4-70	2	188.0	27.3
S9	EN 1.4301	A4-80	3	108.9	25.0
D1	EN 1.4301	A4-70	2	367.5	28.7
D2	EN 1.4301	A4-80	3	179.1	22.5
D3	EN 1.4462	A4-70	2	260.9	33.6
D4	EN 1.4462	A4-70	3	312.5	25.4
D5	EN 1.4462	A4-70	3	382.5	26.0
D6	EN 1.4301	A4-80	2	306.6	31.4
D7	EN 1.4301	A4-80	2	174.3	25.8
D8	EN 1.4301	A4-80	3	181.6	25.3
F1	EN 1.4301	A4-70	1	122.5	33.3
F2	EN 1.4301	A4-70	1	230.9	38.2
F3	EN 1.4301	A4-80	2	180.5	21.8
F4	EN 1.4462	A4-80	2	254.8	29.8
F5	EN 1.4462	A4-80	2	118.4	29.8
F6	EN 1.4301	A4-70	2	147.5	29.0
F7	EN 1.4301	A4-80	2	243.2	35.7
F8	EN 1.4301	A4-70	2	137.1	29.2
F9	EN 1.4462	A4-80	2	130.2	30.8
F10	EN 1.4301	A4-80	2	172.7	21.1

Table 4

Comparison of experimental results with predicted resistances from the existing design methods for type T-S and T-D specimens.

Specimens	Experimental results	Predicted resistances from the existing design methods			
	$F_{u,Exp}$ (kN)	$F_{u,EC3}/F_{u,Exp}$	$F_{u,CSM}/F_{u,Exp}$	$T_{u,AISC}/F_{u,Exp}$	$N_{tu,JGJ}/F_{u,Exp}$
S1	200.2	0.53	0.76	0.87	0.39
S2	106.8	0.61	0.84	1.03	0.50
S3	198.4	0.71	0.77	0.88	0.55
S4	108.9	0.71	0.75	0.85	0.57
S5	161.6	0.39	0.47	0.45	0.29
S6	104.3	0.43	0.76	0.88	0.34
S7	175.2	0.48	0.58	0.54	0.37
S8	188.0	0.43	0.74	0.88	0.31
S9	108.9	0.60	0.83	1.01	0.49
D1	367.5	0.36	0.73	0.78	0.26
D2	179.1	0.56	0.80	0.99	0.43
D3	260.9	0.31	0.38	0.35	0.23
D4	312.5	0.61	0.70	0.76	0.45
D5	382.5	0.65	0.73	0.83	0.46
D6	306.6	0.33	0.68	0.71	0.24
D7	174.3	0.42	0.74	0.88	0.31
D8	181.6	0.55	0.79	0.97	0.42
Mean	-	**0.51**	**0.71**	**0.80**	**0.39**
St. dev	-	**0.13**	**0.12**	**0.19**	**0.11**

Table 5

Comparison of experimental results with predicted resistances from Demonceau et al. **Error! Reference source not found.** for type T-F specimens.

Specimens	Experimental results	Predicted resistances from Demonceau et al. and CSM			
	$F_{u,Exp}$ (kN)	$F_{u,D}$ (kN)	$F_{u,D}/F_{u,Exp}$	$F_{u,CSM}$ (kN)	$F_{u,CSM}/F_{u,Exp}$
F1	122.5	31.5	0.26	61.0	0.50
F2	231.4	54.8	0.24	111.5	0.48
F3	180.7	82.2	0.45	105.1	0.58
F4	255.2	126.7	0.50	139.0	0.54
F5	119.1	43.1	0.36	52.4	0.44
F6	147.5	67.5	0.46	87.9	0.60
F7	243.4	73.1	0.30	130.0	0.53
F8	137.1	53.9	0.39	77.9	0.57
F9	130.5	57.5	0.44	68.5	0.52
F10	173.0	82.2	0.48	105.1	0.61
Mean	-	-	**0.39**	-	**0.54**
St. dev	-	-	**0.09**	-	**0.05**